Electron Transfer Reaction Accompanied by a Structural Change. In the Case of Reaction with $[Ru(NH_3)_5(butyl\ sulfoxide)]^{2+}$ and *cis*-$[Ru(NH_3)_4(pyridine\text{-}4\text{-}carboxamide)_2]^{3+}$

Mitsuru Sano,* Hiromitsu Sago, and Atsuko Tomita

School of Informatics and Sciences, Nagoya University, and Presto21, JRDC, Nagoya 464-01

(Received September 14, 1995)

The oxidation of $[Ru(NH_3)_5(butyl\ sulfoxide)]^{2+}$ by *cis*-$[Ru(NH_3)_4(pyridine\text{-}4\text{-}carboxamide)_2]^{3+}$ has been studied as a case of an electron transfer reaction accompanied by a structural change. Even in an excess of one of the reaction partners, the reaction shows complex kinetic behavior. Treatment of the experimental data points to a mechanism in which the first step is an up-hill electron transfer between the complexes and in which the second step involves isomerization of the unstable sulfoxide complex produced in the first step.

The kinetic and thermodynamic properties of the isomerizations of the $[Ru(NH_3)_5(sulfoxide)]^{3+/2+}$ complexes in acetone were reported[1] as electrochemically, where, in the stable forms, sulfoxide is bound via S to Ru(II)[2] and via O to Ru(III).[3] When the S-bound isomer is oxidized at about 1.0 V,[4] linkage isomerization occurs to the more stable O-bound form. When the resulting species is reduced at about 0.0 V, it rearranges to the more stable S-bound original state, as shown in Fig. 1 for $[Ru(NH_3)_5(butyl\ sulfoxide)]^{2+}$.[1]

We have also reported[5,6] preparation of a complex (1,5-dithiacyclooctane 1-oxide)bis(pentaammineruthenium); its redox behavior is shown in the following scheme (Scheme 1): In these redox processes, there are two intermediate species, $Ru^{2+}S\text{–}SORu^{3+}$ and $Ru^{3+}S\text{–}OSRu^{2+}$, in which the species of $Ru^{3+}S\text{–}OSRu^{2+}$ is formed from oxidation of the species $Ru^{2+}S\text{–}OSRu^{2+}$ and the $Ru^{2+}S\text{–}SORu^{3+}$ is also from reduction of the $Ru^{3+}S\text{–}SORu^{3+}$. Thus each intermediate species forms dependently upon the directions of the redox processes. This demonstrates that the molecule can remember its past. Therefore, we named such behavior "molecular hysteresis". The molecular hysteresis is applicable to make an ultra-high density memory, in which the life time of the memory is important. The life time for the intermediate species was found to be determined with rates of the conversions from one species to another; $Ru^{2+}S\text{–}SORu^{3+} \rightarrow Ru^{3+}S\text{–}OSRu^{2+}$ or $Ru^{3+}S\text{–}OSRu^{2+} \rightarrow Ru^{2+}S\text{–}SORu^{3+}$. This conversion is an electron transfer accompanied by a structural change.

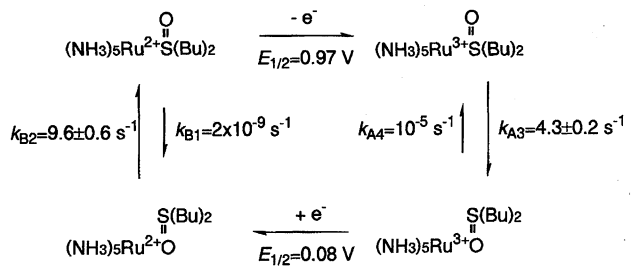

Fig. 1. Redox behavior of $[Ru(NH_3)_5(butyl\ sulfoxide)]^{2+/3+}$ at 20 °C.

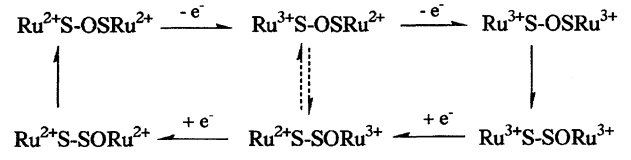

Scheme 1.

A structural change accompanying electron transfer is frequently encountered in biological systems,[7] and the phenomenon constitutes one of the most important aspects of the subject. Hoffman et al.[8] theoretically considered such systems. Despite the importance, few experimental research programs devoted to a systematic investigation of the effect seem to have been undertaken.

On mixing acetone solutions of $[Ru(NH_3)_5(sulfoxide)]^{2+}$ and bisacetonitrileruthenium(III) complexes, a yellow color develops slowly enough that the sulfoxide complex with a redox potential of 0.97 V, S-bound in both oxidation states, can be oxidized by the bisnitrile complex with a redox potential of 0.83 V. This system is an example of electron transfer reaction accompanied by a structural change in homogeneous system, but this is not well suited for study because neither reactants nor products absorb light in a convenient wave length range. Instead we replaced the bisnitrile complex as oxidant by *cis*-$[Ru(NH_3)_4(pyridine\text{-}4\text{-}carboxamide)_2]^{3+}$ (redox potential 0.72±0.01 V) which on $1e^-$ reduction yields a strongly colored product ($\varepsilon = 1.36\times10^4\ M^{-1}\,cm^{-1}$ at 475 nm (1 M = 1 mol dm^{-3})).

In this paper, we study a redox reaction $[Ru(NH_3)_5(butyl\ sulfoxide)]^{2+}$ with *cis*-$[Ru(NH_3)_4(pyridine\text{-}4\text{-}carboxamide)_2]^{3+}$ as a case of an electron transfer reaction accompanied by a structural change.

Experimental

All manipulations and reactions were carried out under Ar.

Materials. $[Ru(NH_3)_5(acetone)](PF_6)_2$ and *cis*-$[Ru(NH_3)_4(acetone)_2](PF_6)_2$ were synthesized from $[Ru(NH_3)_5Cl]Cl_2$ and *cis*-$[Ru(NH_3)_4Cl_2]Cl$ as described in the literature,[9,10] respectively. Dibutyl sulfoxide (buso) were recrystallized from ethylether. Pyridine-4-carboxamide was purchased from Wako Chemical and was used without further purification. Acetone was purified by vacuum distillation over B_2O_3.[11] Anhydrous CH_2Cl_2 was purchased from Aldrich (Sure/Seal bottle) and were used without further purification. Tetra-1-butylammonium hexafluorophosphate (Bu_4NPF_6) (Tokyo Kasei) was twice recrystallized from ethanol and dried at 105 °C under vacuum. All solvents were thoroughly deoxygenated by purging with argon in a Vacuum/Atmospheres Co. inert atmosphere dry glovebox.

$[Ru(NH_3)_5(buso)](PF_6)_2$. Two hundred and twenty milligrams of $[Ru(NH_3)_5(acetone)](PF_6)_2$ was dissolved in 1 mL of acetone. One milliliter of the acetone solution of the sulfoxide (200 mg) was added to the solution of the complex. The solution was stirred for 1 h. The solution was treated with CH_2Cl_2. The resulting pale yellow precipitate was filtered off and the filtrate was treated with CH_2Cl_2. The white solid was filtered off. The solid was redissolved with acetone, and then the solution was again treated with CH_2Cl_2. The precipitate was filtered off, washed with CH_2Cl_2, and dried in vacuo, yield 220 mg (84%). ^{1}H NMR (acetone-d_6) $\delta = 3.65$ (br, 3H, *trans*-NH_3), 3.50—3.37 (m, 4H, CH_2), 2.56 (br, 12H, *cis*-NH_3), 1.90—1.78 (m, 4H, CH_2), 1.54—1.40 (m, 4H, CH_2), 0.97—0.92 (t, 6H, CH_3).

Anal. Calcd for $C_8H_{33}N_5SORuP_2F_{12}$: C, 15.02; H, 5.20; N, 10.95%. Found: C, 15.09; H, 4.95; N, 10.83%.

***cis*-$[Ru(NH_3)_4(pyridine\text{-}4\text{-}carboxamide)_2](PF_6)_2$.** One hundred and sixteen milligrams of $[Ru(NH_3)_5(acetone)](PF_6)_2$ was dissolved in 1 mL of methyl alcohol. One milliliter of methyl alcohol solution of the pyridine-4-carboxamide (260 mg) was added to the solution of the complex, and the mixed solution was stirred for 1 h. The solution was filtered and the filtrate was treated with about 2 mL of CH_2Cl_2 and the resulting red precipitate was filtered off. The filtrate was treated with CH_2Cl_2 and the solid was filtered off. The solid was redissolved with acetone, and then the solution was again treated with CH_2Cl_2. The precipitate was filtered off, washed with CH_2Cl_2, and dried in vacuo, yield 136 mg (88%). ^{1}H NMR (acetone-d_6) $\delta = 8.66$ (m, 4H, py-H), 7.76 (br, 2H, –CONH), 7.68 (m, 4H, py-H), 7.06 (br, 2H, –CONH), 3.19 (br, 6H, *trans*-NH_3), 2.84 (br, 6H, *cis*-NH_3).

Anal. Calcd for $C_8H_{33}N_5SORuP_2F_{12}$: C, 15.02; H, 5.20; N, 10.95%. Found: C, 15.09; H, 4.95; N, 10.83%.

***cis*-$[Ru(NH_3)_4(pyridine\text{-}4\text{-}carboxamide)_2](PF_6)_3$.** One hundred milligrams of *cis*-$[Ru(NH_3)_4(pyridine\text{-}4\text{-}carboxamide)_2](PF_6)_2$ was dissolved in 5 mL of H_2O (pH 1.2). A solution of Ce^{4+} was gradually added to the ruthenium solution until the deep red solution color disappeared. Two grams of NH_4PF_6 was added to the solution and the resulting precipitate was filtered off. The solid was dissolved with 2 mL of acetone. This mixture was stirred for 10 min and then was filtered. The solution was treated with CH_2Cl_2 and the resulting precipitate was filtered off and dried in vacuo, yield 40 mg (33%).

Anal. Calcd for $C_{12}H_{24}N_8Ru_1O_2P_3F_{18}$: C, 16.98; H, 2.85; N, 13.21%. Found: C, 17.25; H, 2.85; N, 12.84%.

Instrumentation and Kinetics. Proton and carbon-13 NMR spectra were recorded on a JEOL EX-270 spectrometer and are reported as ppm shifts from acetone-d_6 (2.04 ppm for ^{1}H and 29.8 ppm for ^{13}C). Cyclic voltammetries were carried out by BAS-100B on acetone solutions of complexes (10 mM) containing 0.20 M Bu_4NPF_6. All potentials are reported vs. the normal hydrogen electrode. The reference electrode was calibrated with the ferrocene–ferrocenium couple ($E_{1/2} = 0.55$ (NHE)) as measured in situ.

The kinetics of the reaction in acetone was monitored spectrophotometrically on a JASCO Ubest-55 spectrophotometer in a thermostated JASCO EHC-441 instrument using quartz cells of path lengths of 1.0 cm with a screw cap fitted with a rubber liner. In the kinetic experiments, a 1 mL acetone solution containing 2.0 mM $[Ru(NH_3)_5(n\text{-butylsulfoxide})]^{2+}$ and 0.20 M Bu_4NPF_6 was placed in the cell and thermostated at the required temperature (20.0±0.1 °C and 10.0±0.1 °C). A 1 mL acetone solution of 0.10 mM *cis*-$[Ru(NH_3)_4(pyridine\text{-}4\text{-}carboxamide)_2]^{3+}$ and 0.20 M Bu_4NPF_6 was stored in a gas-tight syringe in a holder employed a thermostat system with EYELA NCB-2100. After 1 h, the solution was injected to the cell. The cell was shaken to ensure complete mixing, prior to monitoring optical density changes at some appropriate, fixed wavelength. All data were obtained from at least three replicate experiments.

Results and Discussion

The redox potentials for *cis*-$[Ru(NH_3)_4(pyridine\text{-}4\text{-}carboxamide)]^{2+}$, $[Ru(NH_3)_5(buso)]^{2+}$, and $[Ru(NH_3)_5(buso)]^{3+}$ are 0.72±0.01, 0.97±0.01, and 0.08±0.01 V, respectively, in acetone containing 0.20 M Bu_4NPF_6. On mixing acetone solutions of $[Ru(NH_3)_5(buso)]^{2+}$ and *cis*-$[Ru(NH_3)_4(pyridine\text{-}4\text{-}carboxamide)]^{3+}$ complexes, a red color develops in spite of their redox potentials. The kinetics of the reaction was studied using electronic spectroscopy. Figure 2 shows spectral changes for the system at 10 °C; rates for the system are followed by observing the increasing absorption at 475 nm as function of time. Even in an excess of the sulfoxide complex, the reaction does not show a pseudo-first order rate but a complex behavior as shown in Fig. 2b.

For the reaction between $[Ru(NH_3)_5(butyl\ sulfoxide)]^{2+}$ ($Ru^{2+}SO$) and *cis*-$[Ru(NH_3)_4(pyridine\text{-}4\text{-}carboxamide)_2]^{3+}$ (Ru^{3+}), there are two courses, as the following schemes show:

$$\text{Path A}: \quad \underset{(0.97\ \text{V})}{Ru^{2+}SO} + \underset{(0.72\ \text{V})}{Ru^{3+}} \underset{k_{A2}}{\overset{k_{A1}}{\rightleftharpoons}} Ru^{3+}SO + Ru^{2+}$$

$$Ru^{3+}SO \underset{k_{A4}}{\overset{k_{A3}}{\rightleftharpoons}} Ru^{3+}OS$$

$$\text{Path B}: \quad Ru^{2+}SO \underset{k_{B2}}{\overset{k_{B1}}{\rightleftharpoons}} Ru^{2+}OS$$

$$\underset{(0.08\ \text{V})}{Ru^{2+}OS} + \underset{(0.72\ \text{V})}{Ru^{3+}} \underset{k_{B4}}{\overset{k_{B3}}{\rightleftharpoons}} Ru^{3+}OS + Ru^{2+}$$

By path A, $Ru^{2+}SO$ is first oxidized by the Ru^{3+} and the product $Ru^{3+}SO$ isomerizes. On the other hand, by path B, the first step is the linkage-isomerization and the second step is the electron transfer reaction between the $Ru^{2+}OS$ and the Ru^{3+}. We estimated 2×10^{-9} s^{-1} for the rate k_{B1} of the isomerization from the $Ru^{2+}SO$ to the $Ru^{2+}OS$.[1] This shows that isomerization is much too slow to precede electron

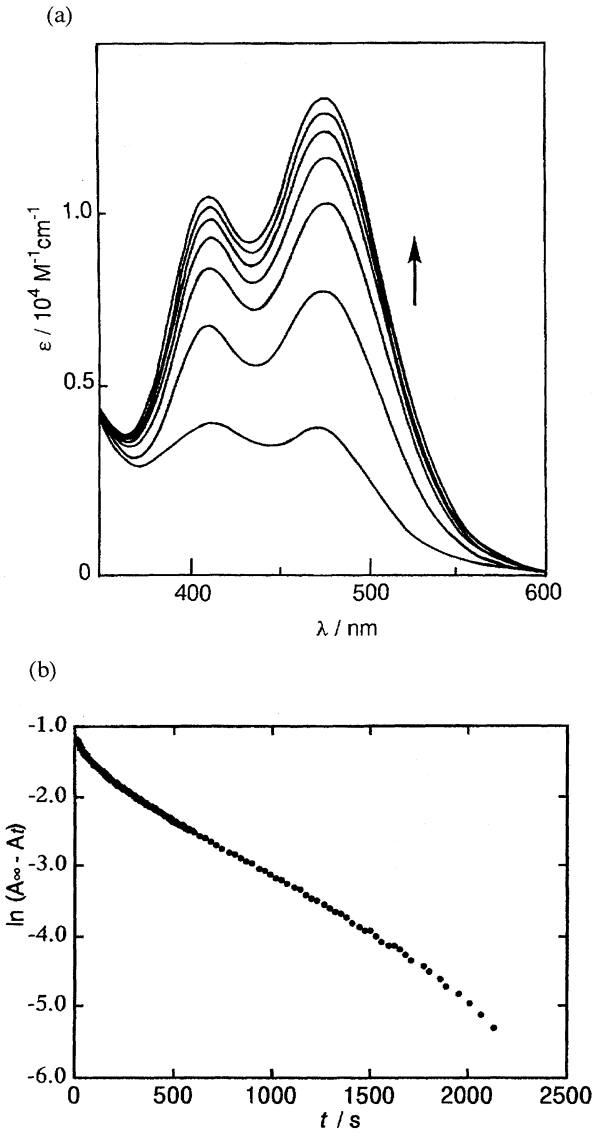

Fig. 2. Visible absorption spectral changes (350—600 nm region) as a function of time for an 1 mL acetone solution of $[Ru(NH_3)_5(\text{butyl sulfoxide})]^{2+}$ (2.0 mM) on addition of a 1 mL of *cis*-$[Ru(NH_3)_4(\text{pyridine-4-carboxamide})_2]^{3+}$ (0.10 mM) at 10 °C. The A_t and A_∞ represent the absorption at 475 nm at times t and ∞, respectively.

transfer in the system under present study and we choose path A as the more probable reaction course.

We will consider a theoretical equation for path A in the reaction. We can get the following equations;

$$\frac{d[Ru^{2+}]}{dt} = k_{A1}[Ru^{3+}][Ru^{2+}SO] - k_{A2}[Ru^{3+}SO][Ru^{2+}] \quad (1)$$

and

$$\frac{d[Ru^{3+}SO]}{dt} = k_{A1}[Ru^{3+}][Ru^{2+}SO] - k_{A2}[Ru^{3+}SO][Ru^{2+}] - k_{A3}[Ru^{3+}SO] + k_{A4}[Ru^{3+}OS] \quad (2)$$

where [ ] denotes concentration of a complex. The species $Ru^{3+}SO$ is an unstable intermediate and application of the steady-state approximation to the equation leads to

$$[Ru^{3+}SO] = \frac{k_{A1}[Ru^{3+}][Ru^{2+}SO] + k_{A4}[Ru^{3+}OS]}{k_{A2}[Ru^{2+}] + k_{A3}}. \quad (3)$$

The data in Fig. 1 show that the half-time for the conversion of the product $Ru^{3+}OS$ to $Ru^{3+}SO$, which is the maximum possible rate for the reverse reaction, is very long compared to the time period of the forward reaction, so that the term $k_{A4}[Ru^{3+}OS]$ can be neglected.

$$[Ru^{3+}SO] \approx \frac{k_{A1}[Ru^{3+}][Ru^{2+}SO]}{k_{A2}[Ru^{2+}] + k_{A3}}. \quad (4)$$

Substituting Eq. 4 for Eq. 1 gives the following equation;

$$\frac{d[Ru^{2+}]}{dt} = k_{A1}[Ru^{3+}][Ru^{2+}SO]\frac{k_{A3}}{k_{A2}[Ru^{2+}] + k_{A3}}. \quad (5)$$

When t=0, $[Ru^{2+}SO]=b$, $[Ru^{3+}]=a$, $[Ru^{3+}SO]=0$, and $[Ru^{2+}]=0$. When $t=t$, $[Ru^{2+}SO]=b-x\approx b$, $[Ru^{3+}]=a-x$, and $[Ru^{2+}]=x$. We can get a following equation;

$$t = \frac{ak_{A2} + k_{A3}}{bk_{A1}k_{A3}}\ln\left(\frac{a}{a-x}\right) - \frac{k_{A2}x}{bk_{A1}k_{A3}}. \quad (6)$$

The difference between the experimental redox potentials (0.25 V=0.97 V−0.72 V) gives $k_{A2}/k_{A1}=2\times10^4$. The observed value of the k_{A3} is 4.3±0.2 s^{-1} at 20 °C.[1] Figure 3A shows simulation curves with Eq. 6 in varying k_{A2}, 10^6 $M^{-1}s^{-1}$, 10^5 $M^{-1}s^{-1}$, and 10^4 $M^{-1}s^{-1}$, by use of above values from experiments with an experimental result at 20 °C. The data have been normalized on the basis of an absorbance after 100 seconds in order to compare the experimental and the theoretical curves. When k_{A2} is 10^6 $M^{-1}s^{-1}$ or more, the simulation curve fits to the experimental one. Figure 3B shows simulation curves with Eq. 6 in varying k_{A3}, 0.43 s^{-1}, 1.8 s^{-1},[12] 4.3 s^{-1}, and 43 s^{-1}, by use of the values, $k_{A2}/k_{A1}=2\times10^4$ and $k_{A2}=10^6$ s^{-1} with an experimental result at 10 °C. The theoretical curve[12] for k_{A3}=1.8 s^{-1} agrees well with the experimental one, a value which is in reasonable agreement with 1.3 s^{-1} obtained for the isomerization rate at 10 °C.[1] Consequently, Eq. 6 can explain the experimental curves.

In order to confirm the approximation of neglecting the term of $k_{A4}[Ru^{3+}OS]$ in Eq. 5, we estimate the values to be 10^{-3} M s^{-1} and 10^{-5} M s^{-1} for $k_{A1}[Ru^{3+}][Ru^{2+}SO]$ and $k_{A4}[Ru^{3+}OS]$ on the 99% completion of the reaction, where the approximation is reasonable.

We conclude that the reaction takes place by path A, where $[Ru(NH_3)_5(\text{butyl sulfoxide})]^{2+}$ is first oxidized by *cis*-$[Ru(NH_3)_4(\text{pyridine-4-carboxamide})_2]^{3+}$ against 24 kJ mol^{-1} up-hill electron transfer with the rate constant over 50 $M^{-1}s^{-1}$ and in the second step the $Ru^{3+}SO$ isomerizes to $Ru^{3+}OS$ with the rate constant of 4.3±0.2 s^{-1} as shown in Fig. 4.

Now we can discuss the life time of the memory in the system of the molecular hysteresis. The life time is determined by the rates of not only the up-hill electron transfer but also the isomerization. In the up-hill electron transfer reaction, the larger the difference of the redox potentials for

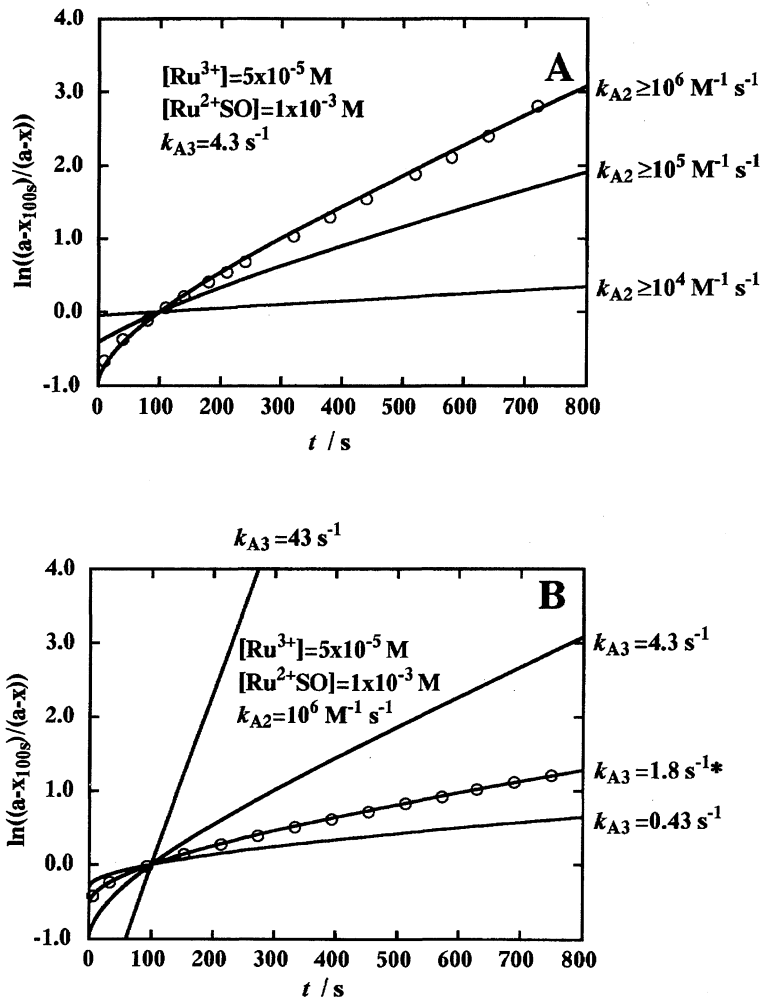

Fig. 3. Theoretical curves on the basis of the path A. The circles for Fig. 3A and for Fig. 3B are the experimental data at 20 and 10 °C, respectively.

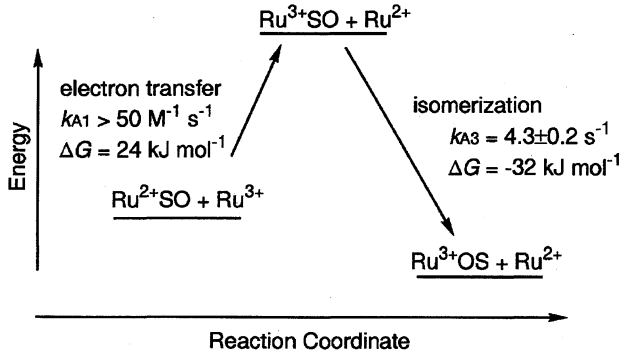

Fig. 4. Energy profile for the electron transfer reaction between $[Ru(NH_3)_5(\text{butyl sulfoxide})]^{2+}$ and *cis*-$[Ru(NH_3)_4(\text{pyridine-4-carboxamide})_2](PF_6)_3$ in acetone at 20 °C.

the $Ru^{2+}SO$ and the Ru^{3+}, the smaller the value of the k_{A1}. Increasing the difference between the redox potentials leads to a molecule with long-life memory.

We turn to a report of Harman and Taube[13] on the reaction of $[Os(NH_3)_5(N,N\text{-dimethylaniline})]^{2+}$ with $[Os(NH_3)_5(CH_3CN)]^{3+}$, which is also an electron transfer reaction accompanied by a structural change. The redox potentials for $[Os(NH_3)_5(CH_3CN)]^{3+}$ and $[Os(NH_3)_5\{\eta^2\text{-PhN}(CH_3)_2\}]^{2+}$ are −0.30 and 0.14 V, respectively. The mechanism proposed for the reaction is as follows; The first step is the $\eta^2 \rightarrow N$ linkage isomerization;

$$[Os(NH_3)_5\{\eta^2 - PhN(CH_3)_2\}]^{2+} \rightarrow [Os(NH_3)_5\{PhN(CH_3)_{2-x}N\}]^{2+}.$$

This reaction was found to be rate-determining step over the concentration range studied, the product being oxidized rapidly by $[Os(NH_3)_5(CH_3CN)]^{3+}$:

$$[Os(NH_3)_5\{PhN(CH_3)_{2-x}N\}]^{2+} + [Os(NH_3)_5(CH_3CN)]^{3+} \rightarrow [Os(NH_3)_5\{PhN(CH_3)_{2-x}N\}]^{3+} + [Os(NH_3)_5(CH_3CN)]^{2+}.$$

The complex with nitrile as ligand is more strongly oxidizing than that with N-bound dimethylaniline by −0.38 V. Harman et al.[14] also found the same mechanism is redox reaction with $[Os(NH_3)_5\{\eta^2\text{-}(CH_3)_2CO\}]^{2+}$ and $[Os(NH_3)_5(PhCN)]^{3+}$.

The mechanism of our reaction corresponds to the reverse (up-hill) reaction in the Harman and Taube system. Both

mechanisms, that of Harman and Taube and ours presented here, are interesting to consider as the mechanism not only for biological and also for "gated"[15] electron transfer systems.

We are grateful to Professor Henry Taube (Stanford University) for his useful discussions and for his encouragement.

References

1) A. Tomita and M. Sano, *Inorg. Chem.*, **33**, 5825 (1994).

2) F. C. March and G. Ferguson, *Can. J. Chem.*, **49**, 3590 (1971).

3) A. Tomita and M. Sano, unpublished result: A single crystal X-ray analysis has been performed for $[Ru(NH_3)_5(dmso)](CF_3SO_3)_3$. The oxygen of the dmso has been confirmed to coordinate to the Ru(III).

4) All potentials quoted are referenced to NHE.

5) M. Sano and H. Taube, *J. Am. Chem. Soc.*, **110**, 5403 (1988); M. Sano, *Kagaku Asahi*, **51**, 34 (1991); M. Sano, *Polym. Adv. Technol.*, **6**, 178 (1994).

6) M. Sano and H. Taube, *Inorg. Chem.*, **33**, 705 (1994).

7) O. Farver and I. Pecht, "Copper Protein," Wiley, New York (1981), pp. 151—192.

8) a) B. M. Hoffman and M. A. Ratner, *J. Am. Chem. Soc.*, **109**, 6237 (1987); b) M. M. Klosek-Dygas, B. M. Hoffman, B. J. Matkowsky, A. Nitzan, M. A. Ratner, and Z. Schuss, *J. Chem. Phys.*, **90**, 1141 (1989).

9) R. W. Callahan, G. M. Brown, and T. J. Meyer, *Inorg. Chem.*, **14**, 1443 (1975).

10) T. Sugaya and M. Sano, *Inorg. Chem.*, **32**, 5878 (1993).

11) D. R. Burfield and R. H. Smithers, *J. Org. Chem.*, **43**, 3966 (1978).

12) The simulation curve for $k_{A3}=1.8\ s^{-1}$ is calculated on the basis of $K=2.8\times10^4$ at 10 °C.

13) W. D. Harman and H. Taube, *J. Am. Chem. Soc.*, **110**, 5403 (1988).

14) W. D. Harman, M. Sekine, and H. Taube, *J. Am. Chem. Soc.*, **110**, 2439 (1988).

15) B. M. Hoffman, M. A. Ratner, and S. A. Wallin, *Adv. Chem. Ser.*, **226**, 125 (1990).